

Interpreting paleoenvironments, subsidence history and sea-level changes of passive margins from seismic and biostratigraphy

Passive margins
Seismic data
Biostratigraphy
Subsidence
Paleoenvironment
Sea level changes

Marges passives
Sismique
Biostratigraphie
Subsidence
Paléoenvironnement
Variations du niveau de la mer

J. Hardenbol^a, P. R. Vail^a, J. Ferrer^b

^a Exxon Production Research Company, P. O. Box 2189, Houston, Texas 77001, USA.

^b Exxon Production Research-European, 213, Cours Victor Hugo, 33321 Begles, France.

ABSTRACT

Interaction between basement subsidence, eustatic sea-level changes, and varying sediment supply shapes the sediment accumulations along passive continental margins. Detailed analysis of the sediments with seismic stratigraphy and well data permits quantification of the subsidence history and reconstruction of paleoenvironments and sea-level changes through time.

The integrated use of seismic stratigraphy and biostratigraphy provides a better geologic age history than could be obtained by either method alone. Paleobathymetry, sediment facies, and relative changes of sea level can be interpreted from seismic data and confirmed or improved on by well control.

Geohistory analysis provides a quantitative analysis of basin subsidence using geologic time-depth diagrams to visualize the total basin subsidence. When this subsidence is corrected for compaction and sediment loading, the thermo-tectonic subsidence is obtained. On passive margins, subsidence is predominantly a result of thermal contraction of the crust and mantle. Long-term eustatic changes are a significant component of the thermo-tectonic subsidence curve. These changes can be quantified by measuring departure from an established set of calculated subsidence curves. Short-term, rapid changes of sea level can be demonstrated from seismic and well data. The stratigraphic resolution of these changes rarely allows exact quantification of their magnitude, but a minimum rate of change of sea level can often be determined. Applications of these procedures are demonstrated with an example from northwest Africa.

Oceanol. Acta, 1981. Proceedings 26th International Geological Congress, Geology of continental margins symposium, Paris, July 7-17, 1980, 33-44.

RÉSUMÉ

Reconstitution des paléoenvironnements, de la subsidence et des variations du niveau de la mer sur les marges continentales passives à l'aide de données sismiques et de la biostratigraphie.

La forme du prisme sédimentaire sur une marge passive résulte de l'interaction entre les variations du niveau de la mer, la subsidence du substratum et les apports sédimentaires. L'analyse détaillée des sédiments à l'aide de la stratigraphie sismique et des données de forages permet de quantifier l'histoire de la subsidence, la reconstitution des paléoenvironnements et les variations du niveau de la mer.

La combinaison de la stratigraphie sismique et de la biostratigraphie améliore la connaissance de l'histoire géologique. La paléobathymétrie, les faciès sédimentaires et les variations du niveau de la mer, interprétés à l'aide de la stratigraphie sismique, sont confirmés ou précisés par les données de forages.

L'analyse géohistorique permet de quantifier la subsidence du bassin à l'aide de diagrammes temps-profondeur. Lorsque cette subsidence est corrigée de l'effet de compaction et de charge des sédiments, on obtient la subsidence thermo-tectonique. Sur les marges passives, la subsidence est essentiellement le résultat de la contraction thermique du manteau et de la croûte. Les variations eustatiques à long terme représentent une importante composante de la courbe de subsidence. Ces variations peuvent être quantifiées en mesurant les écarts par rapport à un ensemble de courbes de subsidence préalablement établi. Les variations à court terme et rapides du niveau de la mer peuvent être démontrées sur les données sismiques et de forages. La résolution stratigraphique de ces changements en permet rarement une quantification, mais un taux minimum de variation du niveau de la mer peut souvent être déterminé. Cette procédure de reconstitution géohistorique est testée sur un exemple de la marge d'Afrique NW.

Oceanol. Acta, 1981. Actes 26^e Congrès International de Géologie, colloque Géologie des marges continentales, Paris, 7-17 juil. 1980, 33-44.

INTRODUCTION

Along passive margins, successions of marine deposits separated by unconformities are commonly found at elevations above present sea level. These sediments were deposited on a slowly subsiding margin while sea level was at a much higher level than at present. In addition to longterm falls or rises of sea level, rapid short-term changes occur that are responsible for the unconformities bounding the marine depositional sequences.

The magnitude of changes in eustatic sea level can be determined from the sedimentary section if the chronostratigraphic and paleobathymetric history can be restored in sufficient detail. Long-term changes in sea level can be estimated from the present elevation of ancient marine deposits after the subsidence history for those deposits is reconstructed. Short-term sea-level changes are in general more elusive, since continuous marine sedimentation during the sea-level change is the exception rather than the rule. Rarely is the entire short-term sea-level cycle recorded in marine sediments laid down in water depths favorable for a high stratigraphic and paleobathymetric resolution.

Eustatic sea-level changes, basement subsidence, and sediment supply are the principal interacting variables in a marine basin (Fig. 1). The interaction is recorded in the sedimentary section deposited in the basin. The resulting depositional sequences, bound by unconformities or their

correlative conformities (Fig. 2), can be recognized in outcrops and wells and on seismic reflection profiles because of important changes in areal distribution, lithology, and depositional environment. Retracing the interaction of eustatic changes and basement subsidence from the sedimentary record is efficiently handled by the geohistory analysis technique. This technique integrates the stratigraphic and paleobathymetric data in a time-depth framework and reproduces the subsidence of basement as a result of basement faulting, crustal and mantle cooling, and sediment loading.

This total subsidence also includes the apparent vertical movement effects of sediment compaction and eustatic sea-level changes. By quantification of the effects of sediment compaction, sediment loading, and thermal subsidence, the eustatic changes can be determined. An example of this analysis shows that in the Early Cenomanian from offshore northwestern Africa, sea level could have been nearly 300 meters higher than the present sea level.

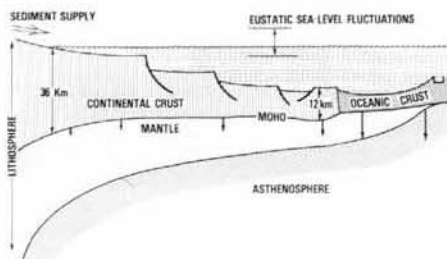


Figure 1
Schematic cross section of a passive margin illustrating the variables controlling the distribution of paleoenvironments and the type of depositional sequence boundaries.

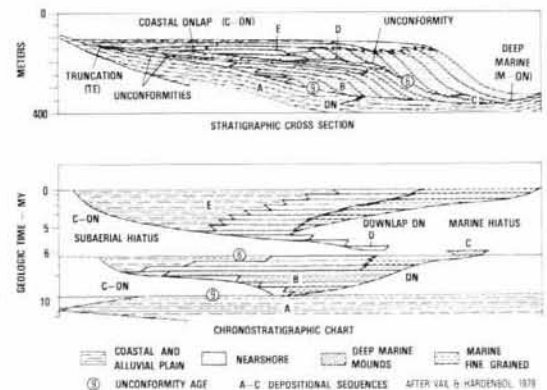


Figure 2
Interaction between basement subsidence and eustatic sea-level changes is recorded in the sediments filling a basin. The upper illustration shows a schematic depth-distance stratigraphic cross section of three sedimentary sequences along a basin margin. The lower figure shows a time-distance or chronostratigraphic reconstruction of the same sedimentary sequences.

The selection of northwest Africa to illustrate the procedure was motivated by the amount and quality of seismic and paleontologic data available. The absence of the Late Cretaceous and Tertiary at the selected well site was offset by the unusual quality of data for the Early Cretaceous and Jurassic section. The older section is much more significant in determining the subsidence history of a margin than the younger section, although a young tectonic event may escape attention.

EUSTATIC SEA-LEVEL CHANGES

Changes in coastal onlap patterns along basin margins are mainly the result of relative changes of sea level (Vail *et al.*, 1977). These relative changes of sea level are in effect produced by the interaction between eustatic changes, basement subsidence, and sediment supply. Without eustatic fluctuations, coastal onlap would be continuous and regular without the downward shifts commonly observed on seismic reflection profiles. Sedimentation would be controlled only by available space, created by basement subsidence, and sediment supply. Quantifying eustatic sea-level changes from measured changes in coastal onlap does not provide an accurate measure, because of variations in subsidence in different basins (Vail *et al.*, 1977). The eustatic sea-level curves from the Tertiary by Vail and Hardenbol (1979) and for the Jurassic through Early Cretaceous by Vail and Todd (1981) are based on estimates from changes in coastal onlap and from paleontological studies. Quantified basement subsidence was not considered for those estimates.

Sedimentary sequences can be viewed in a depth-distance or in a time-distance framework (Fig. 2). Well control, outcrop data, and seismic reflection profiles view the sequences and their unconformable boundaries in a depth-distance framework that does not do justice to the time that is not represented by sediments. If sufficient age data can be obtained, a time-distance record or chronostratigraphic chart can be produced that shows the distribution of the depositional sequences and the extent of the unconformities in space and time.

STRATIGRAPHIC RESOLUTION

A stratigraphic framework that integrates seismic stratigraphic and biostratigraphic information produces a stratigraphic resolution that could not be obtained by either method alone.

Seismic stratigraphy delineates depositional sequences by identifying their boundaries from reflection termination patterns such as downlap, onlap, truncation, and toplap of strata (Mitchum *et al.*, 1977 ; Figures 2, 3). Repeating this procedure for an extensive network of reflection seismic lines defines the sequences and their boundaries over a wide area of varying environments of deposition. This detailed seismic stratigraphic network provides a comprehensive record of relative sea-level changes. The relative magnitudes of a succession of relative sea-level changes can be used to assign tentative ages to the sequences by comparing the succession with one obtained from an area where the stratigraphy is well known. Where possible, however, the predicted seismic stratigraphic ages need to be confirmed by biostratigraphic control.

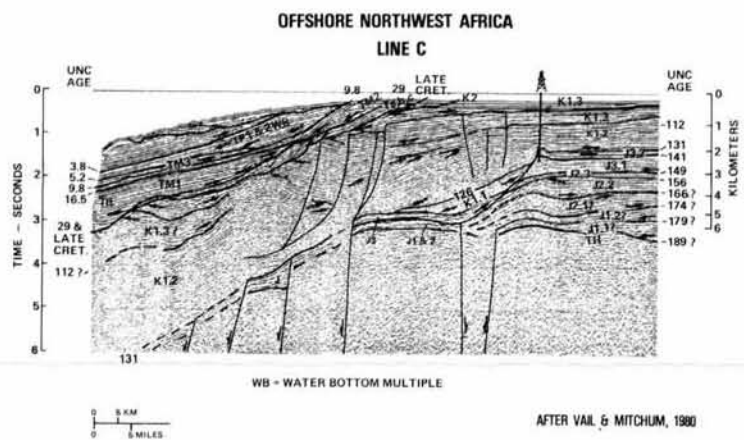
Well control available in the study area needs to be correlated in detail with the seismic stratigraphic network before the biostratigraphic information can be integrated with the seismic stratigraphic framework. If a number of wells are available, the higher resolution biostratigraphy from the deeper water portion of the basins, where more age-diagnostic taxa are found, can be correlated with the basin margin with help of the seismic stratigraphic framework. The area chosen to demonstrate the procedure for determining the magnitude of eustatic sea-level changes is the same offshore northwest Africa area used to document Mesozoic sequences by Todd and Mitchum (1977) and Vail and Mitchum (1980).

PALEOBATHYMETRIC RESOLUTION

Water depth represents the distance between sea floor and sea level and is the portion of the column that is not filled with sediment. Therefore, at any given time, no record of that column is preserved in sediment thickness measurements. The position of the sea floor relative to sea level can, however, be restored from paleontologic and facies records for any significant time horizon in the basin history. Paleobathymetric reconstructions need to be sufficiently detailed (Fig. 4) to give an acceptable accuracy to calculations of the magnitude of eustatic sea-level changes.

Paleobathymetric estimates are based on studies by Bandy (1953), Tipword *et al.* (1966), and Pflum and Frerichs (1976). These studies use the modern depth distribution of mostly foraminiferal taxa as a potential water depth key to

Figure 3
Seismic section from offshore northwest Africa showing interpreted seismic stratigraphic sequences. The sequence boundaries are determined by cycle terminations indicated by arrows. The ages are indicated in millions of years. For sequence designations, see Figure 12.



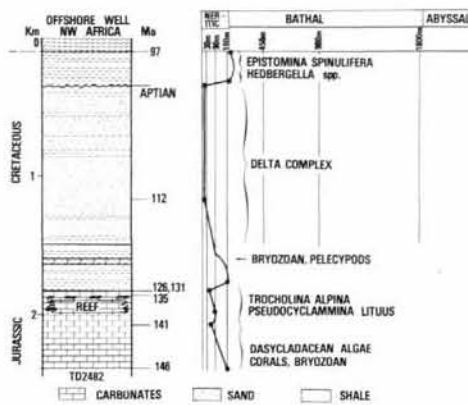


Figure 4 Well section with lithologic, stratigraphic, and paleobathymetric interpretations. The linear paleobathymetric scale indicates decreasing resolution with increasing water depth. The well section shows high paleobathymetric resolution throughout.

fossil occurrences of the same or related taxa. The accuracy of this method seems acceptable for shallow-water deposits of up to 200 m. In deeper environments the resolution decreases rapidly. For a successful study of eustatic changes in sea-level, a well has to be available in a portion of the basin that was filled within 200 m of sea level during eustatic highstands. In such shallow-water conditions, the chronostratigraphic resolution is often rather poor and has to be complemented with ages obtained with seismic stratigraphy.

Facies and paleobathymetric information can also be obtained from the reflection seismic record by careful analysis of the cycle termination at the sequence boundaries and the internal configuration of the sequence (Fig. 5), (Sangree, Widmier, 1977 ; 1979 ; Bubb, Hatlelid, 1977).

GEOHISTORY ANALYSIS

Geohistory analysis is a quantitative stratigraphic technique that combines the stratigraphic and paleobathymetric information in a time-depth framework. The technique in its

modern quantified form was first described by van Hinte (1978), although relative age-depth diagrams were published much earlier (Lemoine, 1911 ; Bandy, 1953). Further improvements, such as corrections for eustatic sea-level changes, sediment compaction, and sediment loading, were added more recently.

Quantitative stratigraphy became feasible with the introduction of reliable time scale models based on a careful integration of biostratigraphy, magnetostratigraphy, seismic stratigraphy, and radiometric dating (van Hinte, 1976 a and b, Jurassic and Cretaceous ; Berggren, 1972 ; Hardenbol, Berggren, 1978, Tertiary). The resulting linear time scale from the base of the Jurassic to the recent is incorporated in the geohistory analysis base form.

Geohistory diagrams show effectively the interaction between sediment supply, eustatic sea-level changes, and basement subsidence through time. Corrections for sediment compaction (Horowitz, 1976) are necessary to obtain a correct total subsidence history. The total subsidence is the sum of all vertical movement and represents the real movement of basement through time. After the effects of sediment loading are subtracted (Horowitz, 1976), a thermo-tectonic subsidence is obtained, which would be the subsidence of basement if no sediment had accumulated in the basin. Crustal cooling and basement-involved faulting are the main components of thermo-tectonic subsidence. Growth faults and salt and shale movements cause anomalies in the thermo-tectonic subsidence curve but do not affect its real magnitude. After allowances are made for anomalies caused by faulting and/or mobile substrata, the curve can be compared with one of a number of crustal subsidence curves for different amounts of lithospheric injection modified after the dike injection model (Fig. 6) of Royden *et al.* (1980). The stretching model of the same authors did not match the Early and Middle Jurassic subsidence observed at the well site. Matching the thermo-tectonic data points with one of the dike injection model curves allows quantification of the thermal component of the observed subsidence history, independent of anomalies caused by eustatic sea-level changes and inaccuracies in chronostratigraphic and paleobathymetric interpretations.

CONSTRUCTION OF GEOHISTORY DIAGRAM

To construct a geohistory diagram (Fig. 7), first a paleobathymetric interpretation for each stratigraphic datum is plotted below the present sea level. The line connecting these points represents the paleobathymetric history through time. The stratigraphic information for a given location, gathered from all available sources, is entered in a stratigraphic column, which shows the subdivisions and thicknesses as they are encountered at present in a well or on a reflection seismic line. This stratigraphic information is also entered in the diagram and plotted against the linear time scale beginning with the base of the Sinemurian (189 Ma), which is the oldest horizon that can be correlated within the area. The underlying Hettangian was at the surface just before the first marine sediment was laid down. If the first sediment is nonmarine, an elevation relative to sea level at that time remains unknown. At each subsequent datum the base of the Sinemurian is plotted at the depth it reached below the sea floor at that time as a result of basement subsidence amplified by sediment loading. The sediment columns above the Hettangian are restored to their original depositional thickness. The line connecting the

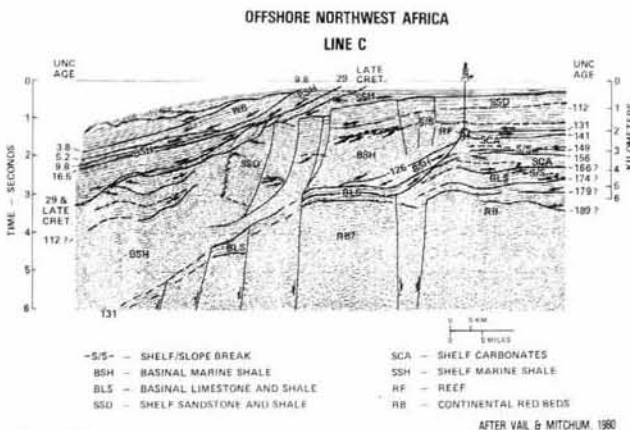


Figure 5 Seismic section from offshore northwest Africa showing interpreted seismic stratigraphic sequences with seismic facies interpreted from the nature of the sequence boundaries and the internal reflection characteristics within the sequence. For sequence designations, see Figure 12.

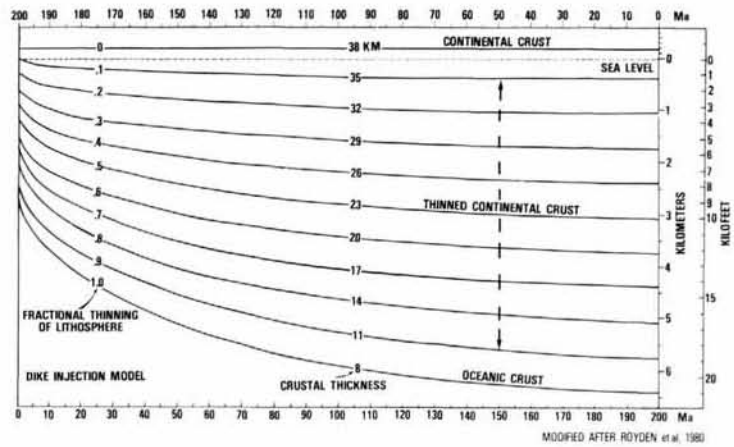


Figure 6
Subsidence curves showing the relationship between subsidence and injection of the lithosphere for the dike injection model modified from Royden et al. (1980).

basal Sinemurian depth plots depicts the total subsidence of basement that occurred at this location from the earliest Jurassic to the present.

The correction for sediment compaction with depth of burial is lithology dependent. Lithologies for the section for which the geohistory diagram is made are determined from well samples and well logs. Lithologies for the section below the total well depth are determined from seismic data. The Cenomanian through Hauterivian section is predominantly clastic. The compaction for shales is determined with $\varnothing Z = \frac{0.7}{1 + 0.0017}$ (Horowitz, 1976) and for sand with $\varnothing Z = 0.38 e^{-5 \times 10^{-3}}$ (D. H. Horowitz, pers. comm., 1980), where \varnothing is porosity and Z is depth in meters.

The Berriasian through Sinemurian section consists of different types of carbonate rocks. Reef carbonates are

assumed to undergo minimal compaction comparable to the porosity reduction of sand. Grain carbonates are assumed to compact like sand containing 30% shale, and micrites like shale containing 35% sand.

SEDIMENT LOADING CORRECTIONS

Subsidence resulting from sediment loading represents an important portion of the total subsidence observed anywhere in a sedimentary basin. Since sedimentation is a function of sediment supply and available space, sediment fill histories can be highly variable depending on the position in the basin. For meaningful comparisons of subsidence histories between different locations within a basin, the effect of differences in sediment fill histories has to be eliminated.

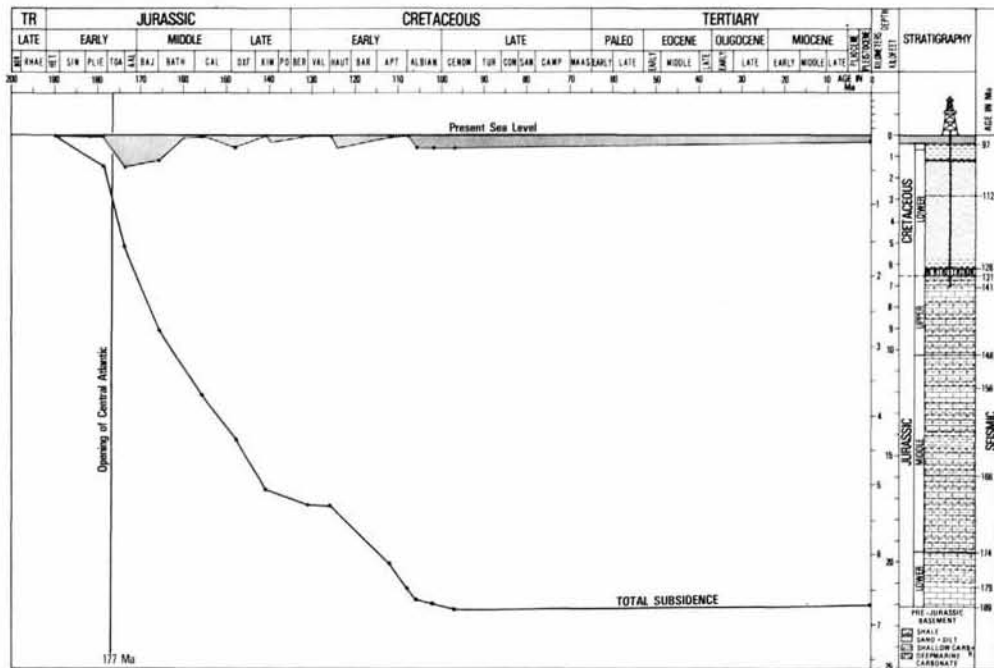


Figure 7
Geohistory analysis diagram with stratigraphic and paleobathymetric histories for a combined well and seismic location. The total subsidence curve depicts the subsidence of the Early Jurassic base through time.

An isostatic loading model assuming an Airy type crust (Horowitz, 1976) seems to be adequate for a loading correction in most basins as long as sediments are more or less uniformly distributed (Fig. 8). In areas adjacent to localized depocenters, such as major deltas building out in deep water or along compressional plate boundaries, an isostatic correction is not sufficient and a flexural loading model should be used (Watts, Ryan, 1976). With a sediment density of 2.7 g/cm³ (at zero percent porosity), the mantle displacement as a result of sediment loading is 0.726 times the thickness of the solid sediment column.

The subsidence resulting from sediment loading is subtracted from the total subsidence in the geohistory diagram. The points thus obtained show the subsidence of the basal Sinemurian if no sediment had been deposited and only water had filled the basin. This resultant curve is the thermo-tectonic subsidence curve (Fig. 9), which shows mostly the effect of cooling of the crust and mantle, but

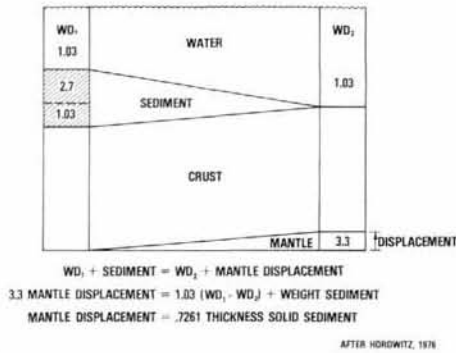


Figure 8
Isostatic backstripping model for Airy type crust.

effects of eustatics, faulting, and salt or shale movement should be identified if present.

Thermo-tectonic subsidence combines the effects of cooling of the crust and mantle and of tectonics such as basement-involved faulting and mobile salt and shale. The tectonic effects will, however, vary much more from place to place within a basin than the effects of crustal cooling. Constructing a number of thermo-tectonic curves for different locations in a basin will facilitate the distinction between thermal and tectonic subsidence. A detailed familiarity with the geologic history of the basin will further help in the distinction. The type of basin is another important factor in the interpretation. Passive margins with a single crustal thinning event, such as the Atlantic margin off northwest Africa, are dominated by tectonic subsidence during the initial rifting, but soon after the formation of the first oceanic crust, the subsidence becomes entirely contraction unless interrupted by a tectonic event.

ESTIMATE OF LONG-TERM EUSTATIC SEA-LEVEL CHANGES

The thermo-tectonic subsidence curve for the offshore northwest Africa example shows a high subsidence rate during the Early Jurassic that rapidly decays to a much slower rate in the Cretaceous and Tertiary (Fig. 9). The general shape of the curve resembles the exponential subsidence curves resulting from crustal and mantle cooling (Royden *et al.*, 1980), even though the positions of the data points in the example are affected by eustatic changes of sea level.

The initial rifting phase along the northwest African margin probably started in the Triassic, whereas the age of the earliest oceanic crust is generally quoted as 180 Ma (Pitman,

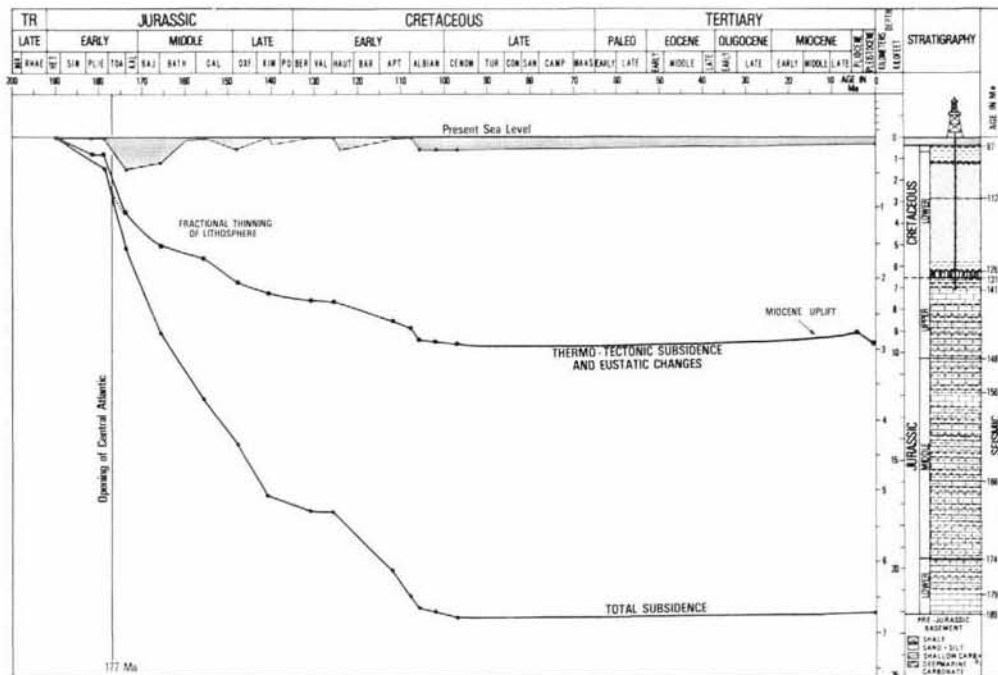


Figure 9
Geohistory diagram showing the thermo-tectonic subsidence curve of the base independent of sediment loading. Depicting the subsidence of the Early Jurassic base if the basin was not filled with sediment. A small compressional uplift is assumed for the Late Tertiary.

Talwani, 1972 ; Hayes, Rabinowitz, 1975). The earliest magnetic anomaly is M 26 at 153 Ma, but the presence of a magnetic quiet zone does not preclude an earlier onset of spreading. Seismic stratigraphic and seismic facies studies support an Early Jurassic opening because of indications of Late Pliensbachian to Toarcian deeper water deposits in the area. Although the rapid subsidence in the Early Jurassic could have a minor tectonic component, most of the constructed curve is the result of crustal and mantle cooling, albeit with a clear influence from the long-term eustatic change in sea level.

The history of relative changes of coastal onlap suggests (Vail *et al.*, 1977) that eustatic sea level underwent considerable changes in the Mesozoic and Cenozoic. Their study shows that in the Early and early Middle Jurassic, sea level was close to the present sea level. A major rise began in the Callovian (156 Ma) and, with short interruptions in the Valanginian, Aptian, and Cenomanian, continued into the Late Cretaceous. This general rise of sea level from Late Middle Jurassic to Late Cretaceous has a steepening effect on thermo-tectonic subsidence curves that are not corrected for eustatic changes. This eustatic effect complicates the comparison between reconstructed thermo-tectonic curves and model curves for crustal and mantle thermal subsidence (Royden *et al.*, 1980).

If sea level in the Early and Middle Jurassic was as close to the present sea level as is suggested by the magnitude of relative changes of coastal onlap, the data points for that portion of the section should match one of the model curves for crustal and mantle cooling. This assumes that the observed thermo-tectonic subsidence curve represents only thermal subsidence with long-term eustatic departures that started immediately after the formation of the first oceanic crust. The geohistory diagram (Fig. 10) suggests that the first oceanic crust was formed at 177 Ma between the

179 Ma and 174 Ma sequence boundaries. The model curve for a 60% injection of the lithosphere matches the Early and Middle Jurassic data points (Fig. 10). All other data points beginning in the Late Jurassic fall significantly below the 60% model curve, which is consistent with a general rise in eustatic sea level in the Late Jurassic and Early Cretaceous.

Other model curves, such as those for 50% and 40% injection of the lithosphere, do not match the steep initial portion of the constructed curve. These two model curves indicate an initial thermal subsidence for an opening event at 177 Ma that is less than the observed total subsidence.

The present-day data point in the geohistory diagram (Fig. 10) falls about 100 m above the 60% model curve. This is interpreted as the result of Late Tertiary uplift, which can be substantiated by several lines of evidence. Compressional tectonics associated with the formation of the High Atlas Mountains may have begun in the Late Oligocene and continued through the Late Miocene, resulting in significant erosion of older deposits. Only the clinoform toes of the Middle Miocene sea-level highstand sequences are preserved (Fig. 3). Toplap associated with the Pliocene highstand sequence seaward of the well location suggests that the Cenomanian at the well site was at or slightly above sea level at that time. The subsidence of the Cenomanian surface since the Middle Pliocene can be estimated at 177 m if we add Middle Pliocene eustatic sea level (+ 80 m, Vail, Hardenbol, 1979) and present-day water depth (97 m). This subsidence is faster than the thermal contraction from an Early Jurassic opening event as is suggested by the 60% model curve. By the end of the Miocene the total compressional uplift may have exceeded 200 m (Fig. 10).

Independent qualitative evidence for an uplift is provided by seismic interval velocities that suggest that the Early Cretaceous sediments are overcompacted for their present burial depth. The observed interval velocities require a

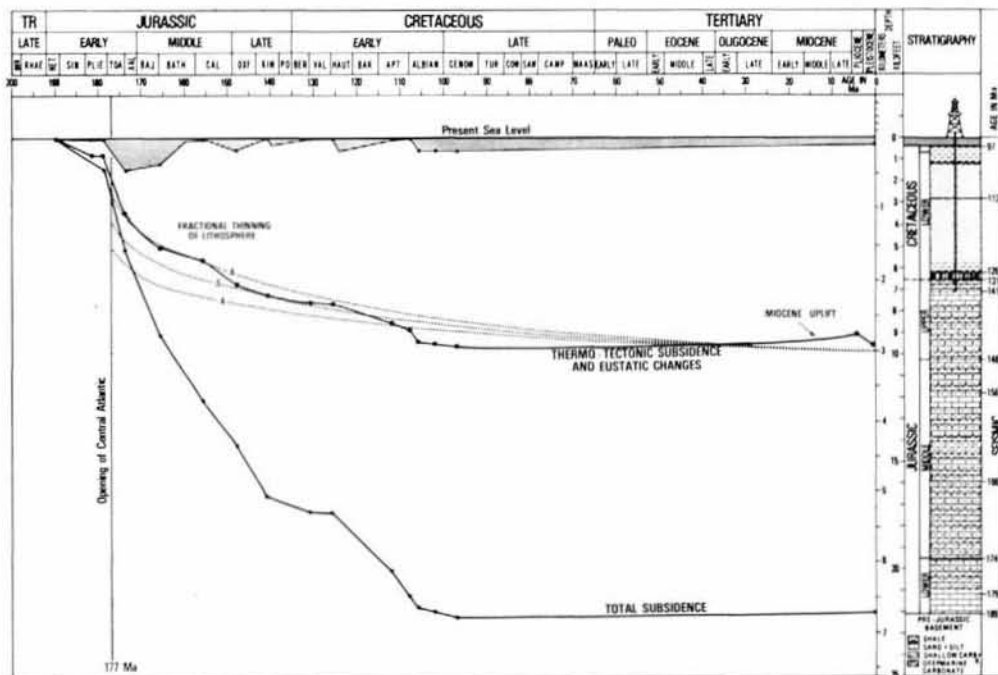


Figure 10 Geohistory diagram comparing thermo-tectonic subsidence with model curves for three different amounts of injection of the lithosphere. A small compressional uplift is assumed for the Late Tertiary.

burial depth between 450 and 750 m some time between the Cenomanian and the present. Without an uplift this burial depth could have been accomplished only if the basin at the well site was filled to sea level in the Late Cretaceous and subsequently eroded during lowstands in the Tertiary, especially in the Late Oligocene. All Upper Cretaceous and Lower Tertiary deposits encountered in the area are deposited in bathyal water depths, and the configuration of the seismic sequences suggests that the basin at the well site was not filled to sea level until the Oligocene. Several lines of evidence seem to agree that at least some uplift occurred in the Late Tertiary. The amount of uplift cannot be determined with accuracy because the Tertiary stratigraphic information is very incomplete as a result of the uplift. In the calculations for eustatic sea-level changes a 100 m uplift is used. This value is estimated from the position of the present-day data point relative to the 60% model subsidence curve in Figure 10. The resulting values are compared with those obtained if no uplift is taken into account.

The distance between the thermo-tectonic subsidence curve and the 60% model subsidence curve in Figure 10 is a measure of the long-term eustatic sea-level change in the Jurassic and Early Cretaceous. Sea level is rising in the late Middle Jurassic and begins falling in the latest Jurassic and Berriasian. A new sea-level rise begins in the Hauterivian or mid-Valanginian and continues into the Early Cenomanian. Measuring eustatic changes directly from Figure 10 produces values that require correction for the loading effect of eustatic sea-level changes as follows :

$$MD = \Delta \text{Sea level} + \frac{\rho_w}{\rho_m} \times \Delta \text{Sea level} = 1.309 \Delta \text{Sea level}$$

or $\Delta \text{Sea level} = \frac{MD}{1.309}$, where MD is the measured distance of the data point below the model subsidence curve in Figure 10.

The calculation of long-term eustatic sea-level changes is based on an isostatic comparison on an Airy type crust (Horowitz, 1976 ; Watts, Ryan, 1976). At 97 Ma (Early Cenomanian) depositional water depth as determined from benthonic microfossils is 180 m. Early Cenomanian beds are still (or again) at the sea floor covered by 97 m of water.

The isostatic comparison is given by the equation :

$$WD_1 + Ts = WD_2 + EF + MC + Ru \quad (1)$$

where WD_1 is the original water depth, Ts is the thermal subsidence from the 60% model curve in Figure 10, WD_2 is the present water depth, EF is the eustatic difference, MC is the mantle compensation after a eustatic change, and Ru is the present-day expression of the regional uplift in the Late Tertiary (100 m). The effects of mantle compensation can be determined by the equation :

$$MC = EF \frac{\rho_w}{\rho_m - \rho_w} = 0.45 EF, \quad (2)$$

where ρ_w is the density of seawater (1.03 gr/cm³) and ρ_m is the average density of the mantle (3.33 gr/cm³). Equation (1) can be written as :

$$EF = \frac{(WD_1 - WD_2) + Ts - Ru}{1.45} \quad (3)$$

Substituting values for the Early Cenomanian and the present in equation (3) results in an apparent eustatic sea-level fall of 281 m (Fig. 11). Equation (3) calculates

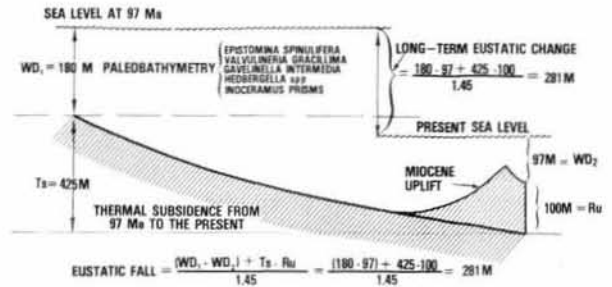


Figure 11
Calculation of eustatic sea-level change from the Early Cenomanian to the recent.

eustatic sea level change for water-filled basins only. For other data points in the Early Cretaceous and Jurassic additional corrections are required for sediments deposited during the respective time intervals. Isostatic comparisons can be made by removing the sediment and restoring the water depth as follows :

$$EF = \frac{WD_1 - (WD_2 + WR) + Ts - Ru}{1.45} \quad (4)$$

where WR is the restored water column after backstripping and taking into account unloading adjustments and porosity restoration of the underlying section. The apparent sea-level changes for data points in the Early Cretaceous, Late Jurassic, and Middle Jurassic determined in several different ways are listed in the Table. The eustatic changes were initially calculated for an assumed uplift of 100 m and for the case that no uplift occurred. The values measured in Figure 10 and corrected for eustatic water loading should agree with the calculated values if no uplift occurred. The Table shows that the measured values fall between those calculated for a 100-m uplift and for no uplift, thus confirming some uplift but not as high as 100 m. If the present-day data point on the thermo-tectonic curve were 70 m above the model curve there would be close agreement between calculated and measured eustatic sea-level changes.

The eustatic sea-level values thus obtained represent the highest sea-level stand in each sequence. The changes observed are therefore predominantly changes in the long-term eustatic sea level. There is close agreement with previous results obtained by different methods by Vail *et al.* (1977), Vail and Todd (1981), Hays and Pitman (1973), and

Table

Eustatic sea level in meters above the present sea level calculated with equation (4) for three different amounts of Late Tertiary compressional uplift compared with the eustatic sea level measured from the geohistory diagram in Figure 10 (corrected for eustatic highstand loading effects). Figures for the 70 m uplift are the preferred values.

Age	No uplift	100 m uplift	70 m uplift	From Fig. 10
Early Cenomanian	350	281	302	302
Late Albian	359	290	311	306
Top Aptian	259	190	210	206
Middle Aptian	195	126	147	138
Top Valanginian	129	60	81	69
Top Berriasian	179	110	130	107
Mid-Kimmeridgian	247	178	199	149
Top Callovian	210	141	162	107
Top Bathonian	77	8	29	0

Pitman (1978). A significant difference exists, however, with the values obtained by Watts and Steckler (1979) using a similar method based on the subsidence history of the Atlantic margin of the North American east coast. A possible explanation for their much lower results is that their assumption of the thermo-tectonic subsidence of the Atlantic margin being a single thermal contraction event is not valid. Thermo-tectonic subsidence histories for Georges Bank and Baltimore Canyon COST wells suggest considerable tectonic activity in the Early Cretaceous and Middle Tertiary.

IDENTIFICATION OF SHORT-TERM EUSTATIC CHANGES

Previous sections of this paper discussed the paleoenvironments, subsidence history, and long-term sea-level changes determined from a well located on seismic line C, offshore northwest Africa. The well log and seismic section show that there are many abrupt vertical changes in depositional environments and lithofacies. In order for these abrupt changes to occur, a rapid change is necessary in one or more of the three variables : rate of subsidence, rate and type of deposition, or rate of eustatic sea-level changes. Figure 10 shows that subsidence in the area of the well follows a normal thermal contraction curve from the time of initial formation of oceanic crust (± 177 Ma) to the Late Oligocene, when uplift associated with the High Atlas Mountains commenced. All changes in subsidence are gradual except for the initial subsidence following the formation of oceanic crust in the Atlantic (± 177 Ma) and the subsidence following the uplift associated with the High Atlas (± 3.8 Ma). The type and rate of deposition of the sediments in the

northwest African margin also change through time. These changes are, however, gradual when the total basin is studied. In any one location, abrupt changes in sediment type and sedimentation rate are common occurrences. Global studies of the Jurassic and Tertiary (Vail *et al.*, 1977 ; part 4, Fig. 6 ; Vail, Todd, 1981 ; Vail, Hardenbol, 1979) show that rapid eustatic sea-level changes occur periodically (Fig. 12). The timing of these global changes coincides with the changes observed in northwest Africa. We conclude that most of the abrupt changes observed in the well and on seismic line C are caused by these rapid changes in eustatic sea level.

Three types of eustatic changes that cause unconformities can be distinguished : 1) rapid falls of eustatic sea level usually greater than the rate of subsidence ; 2) slower falls of eustatic sea level commonly less than the rate of subsidence in basins with significant subsidence ; and 3) rapid rises of eustatic sea level.

Rapid rates of fall of eustatic sea level are characterized by unconformities associated with subaerial exposure on the shelf, canyon cutting, submarine erosion, lowstand deltas and fans, and shifts in submarine depositional patterns where fans and lowstand deltas are absent (Fig. 13). Slow falls less than the rate of subsidence are similar except that the outer portion of the shelf may not be subaerially exposed and lowstand deltas, fans, and canyon cutting are rare. Marine regressions commonly underlie these types of unconformities. Rapid rises are commonly associated with marine transgressions. Basal transgressive deposits overlain by local submarine unconformities may be present (Vail, Todd, 1981).

The following paragraphs will describe the stratigraphy and facies of the well and seismic line C (Fig. 5) and discuss what may have caused the abrupt changes in depositional

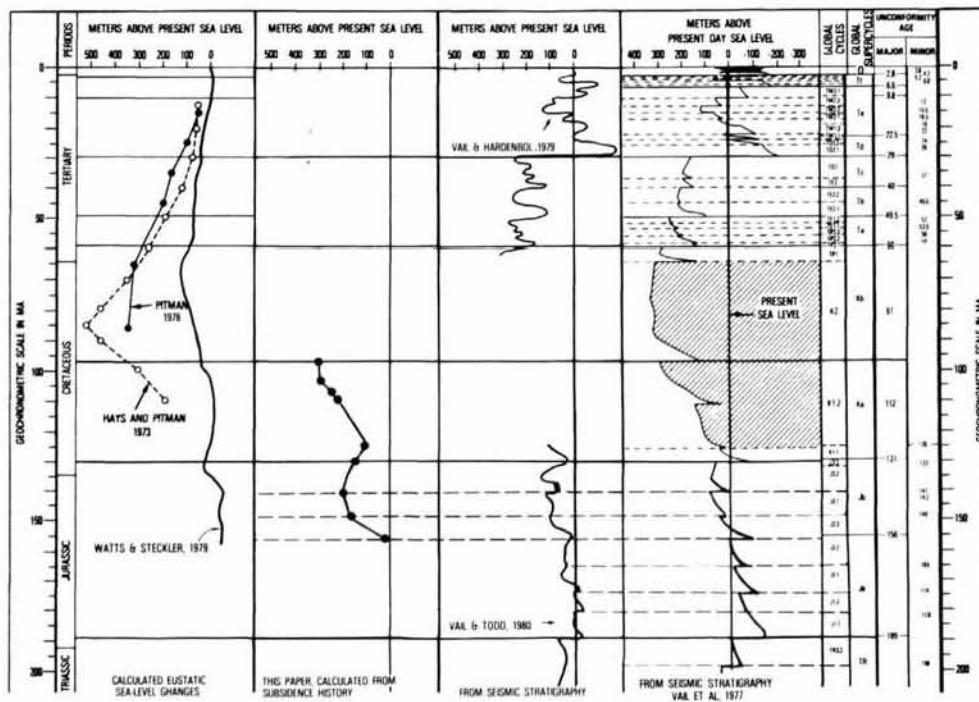


Figure 12 Comparison of eustatic sea-level changes determined from the subsidence history of the northwest African margin with previously published estimates for global changes of sea level.

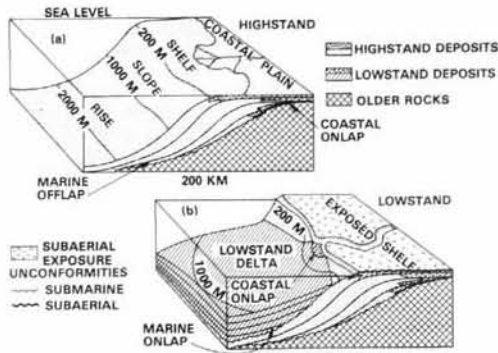


Figure 13
Depositional patterns during highstand (a) and lowstand (b) of sea level.

environments and lithofacies. Seismic line C is used to illustrate these changes for the Mesozoic section. Two seismic lines shown on Figure 14 are used for the Tertiary and Cretaceous.

The first major abrupt vertical change occurs at an unconformity labeled 189 ? Ma on Figure 5. On other seismic sections this unconformity can be traced across the shelf close to a well drilled on land near the coastline (Vail, Mitchum, 1980), where Middle to Late Jurassic clastics overlie the unconformity and Hettangian-Triassic continental red beds underlie it. These beds are locally truncated. To the south the unconformity can be traced below a thick salt section. Well data to the south show that an interval of shallow-water carbonates, anhydrites, and variegated shales, dated by biostratigraphy as probably Early Jurassic, overlie the salt. Seismic correlations indicate that the onlapping reflections between sequence boundaries 177 Ma and 189 Ma (on line C, Fig. 5) correspond to this interval. The unconformity is believed to correlate with the basal Sinemurian (189 Ma) unconformity. In the area of study it marks an abrupt change from continental red beds to a marine section containing salts, anhydrites, and carbonates. It is interpreted on the basis of global studies to be caused by a rapid fall and rise of eustatic sea level that occurred in the Early Sinemurian (between the *Arietites bucklandi* and *Arnioceras semicostatum* ammonite zones, A. Hallam, pers. comm., 1981).

The next abrupt vertical change is best observed on seismic data, such as line C, Figures 3 and 5. It occurs at the sequence boundary labeled 179 ? Ma and is marked by

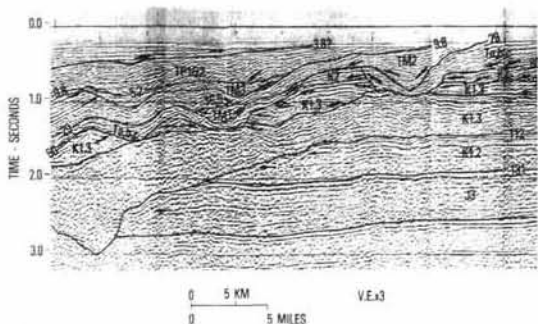


Figure 14 a
Seismic line parallel to shelf edge, offshore northwest Africa, showing major erosional patterns in the Early Cretaceous and Tertiary. For sequence designations, see Figure 12.

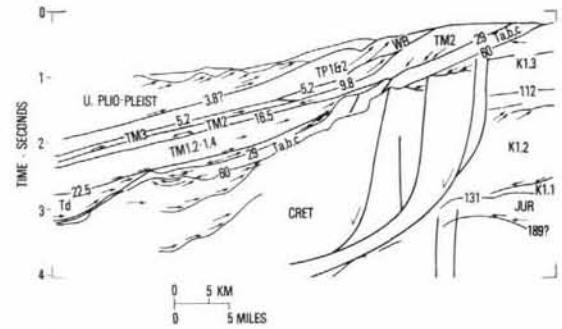


Figure 14 b
Seismic line perpendicular to the shelf edge, offshore northwest Africa, showing major erosional patterns in the Tertiary. For sequence designations see Figure 12.

downlap over parallel reflections. The downlap is interpreted as the toes of prograding clinoforms. The relief of these clinoforms indicates upper bathyal paleowater depths. This boundary is interpreted as an abrupt change from shallow-water carbonates, variegated shales, and evaporites to deep-water carbonate muds. Well data to the south document a change from the shallow-water carbonates and evaporites to massive micritic limestones, but no fossils were identified to verify the deep-water interpretation of this interval. The sequence boundary is correlated with the global fall and rise of eustatic sea level that occurred within the early part of the Late Pliensbachian at 179 Ma. Paleontologic data from wells within the area were undiagnostic and could only be dated as probably Early Jurassic. The rapid deepening and landward shift of the shelf edge is believed to be related to the increased rate of subsidence following the formation of oceanic crust to the west.

The next major abrupt vertical change is well documented by wells as a change from Bathonian shelf carbonates to upper bathyal Callovian shales. Seismic data show a continuous high-amplitude reflection on the shelf with evidence of truncation at the shelf edge. The sequence boundary labeled 156 Ma on Line C (Fig. 5) indicates the abrupt change from carbonate to shale. Landward, this sequence boundary can be traced on seismic data below a prograding sequence that is verified in a well as Callovian marine shale (Fig. 15). The relief on the clinoforms, shown on this

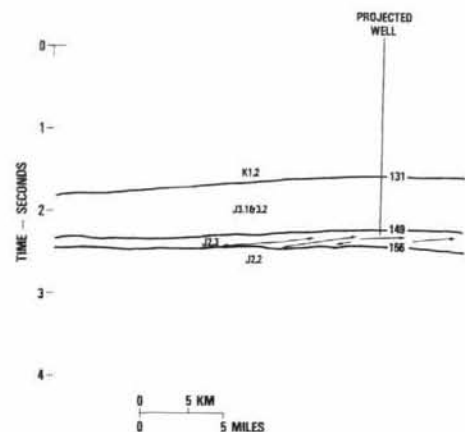


Figure 15
Offshore northwest Africa seismic line showing prograding Callovian shelf margin. For sequence designations see Figure 12.

section, indicates water depths of approximately 300 m. The rapid change from shallow shelf to upper bathyal water depths (± 50 to 300 m) from the Bathonian to the Callovian must have taken place early in the Callovian, since the seismic patterns indicate mainly progradation during the Callovian. This water-depth change of 250 m probably occurred in not more than 2 to 4 million years, during which time the thermo-tectonic subsidence of 23 m/Ma (Fig. 6, 10) would amount to 45 to 90 m. Between 160 and 200 m of the water-depth change must have been caused by a rise of eustatic sea level in 2 to 4 million years, which requires rates of eustatic rise from 4 to 10 cm per 1,000 years and could be much more rapid.

The next major abrupt vertical change is also well documented by well control and occurs between Berriasian shallow-water shelf carbonates and upper bathyal (200-250 m) Hauterivian shale on the shelf, and between Berriasian deep marine micritic carbonates and Valanginian reddish brown deep marine mudstones in the basin. The well on the shelf edge encountered a 6.3-meter cavern, the base of which was 70 m below the top of the Berriasian carbonate. The sequence boundary labeled 131 Ma on line C (Fig. 3,5) marks this change. The Valanginian sequence is shown as a slopefront-fill seismic facies pattern seaward of the shelf edge reef encountered in the well. The Valanginian unit (126-131 Ma) is interpreted as the edge of a lowstand delta diagrammatically illustrated in Figure 13. It indicates that sea level fell below the shelf edge at the beginning of Valanginian time. The karst cavern drilled in the well is also evidence for a sea-level fall at this time. Since the thermo-tectonic subsidence in the Valanginian was 0.99 cm per 1,000 years (Figs. 6, 10), sea level must have dropped at a greater rate to fall below the shelf edge. The lowest marine shales overlying the Berriasian carbonates are dated as Hauterivian. The above observations are interpreted as indicating a rapid rise of sea level during the Valanginian of at least a few cm per 1,000 years following a fall that exceeded 1 cm per 1,000 years. The magnitude of the fall cannot be estimated from these data, but studies from other areas indicate it may approximate 100 m. The water-depth increase over the shelf is approximately 200 m. The subsidence curves (Fig. 6, 10) indicate 47 m were due to thermo-tectonic subsidence and thus 153 m must be due to eustatics rising at a rate of 3 to 8 cm/1,000 years. The amount of rise over the upper slope must be added to this to obtain the total rise, but it cannot be determined from the available data.

The Hauterivian-Aptian interval consists of a large upward-coarsening, prograding delta. A rapid fall and rise of sea level within this delta is indicated by a large canyon cut, shown on Figure 14 a, which is dated as occurring within the Mid-Aptian (112 Ma). Upper bathyal Middle Albian shales overlying the delta indicate a rise in sea level at this time.

Evidence of many other rapid changes of sea level is shown in Figure 14. Slope-front-fill facies of Late Oligocene-Early Miocene (29-16.5 Ma), Late Miocene (9.8 Ma), and Late Pliocene (3.8 Ma), together with their underlying unconformities showing erosional truncation, indicate lowstands. Prograding units and their equivalent deep marine draping shale, such as the Middle Miocene (16.5-9.8 Ma) and Early-Middle Pliocene (6.6-3.8 Ma), indicate highstands.

The present flooded shelf is believed to be due to subsidence following the Miocene uplift associated with the High Atlas Mountains. A widespread truncated surface marks the erosions of tilted beds following that uplift.

DISCUSSION

The magnitude of long-term sea-level changes between the Early Cretaceous and the present, as determined from the subsidence history of a basin offshore northwest Africa, is in line with previously published estimates. Values obtained by Hays and Pitman (1973) and Pitman (1978) for the mid-Cretaceous from rates of ocean spreading and by Vail and Todd (1981) for the Jurassic and earliest Cretaceous are very close to the estimates in this paper. They exceed, however, the values obtained by Watts and Steckler (1979), using a similar method based on margin subsidence.

The models and assumptions used in this study are tentative and require further evaluation and improvements. However, repeating this method for a number of passive margins with adequate stratigraphic and paleobathymetric control should demonstrate trends in the magnitude of long-term eustatic sea-level changes. Short-term changes in sea level can be determined from detailed studies within a quantified framework of subsidence and long-term eustatic sea-level changes. Rates of change of the short-term sea-level fluctuations may be readily determined in areas with detailed age and paleobathymetric control. The magnitude of short-term sea-level changes is much more difficult to estimate.

Acknowledgements

We are grateful to R. M. Mitchum and C. R. Tapscott for reviewing the manuscript and suggesting improvements. D. H. Horowitz and C. R. Tapscott provided valuable assistance in solving problems with the compaction, loading, and subsidence models. We thank our colleagues in Houston and Bordeaux, France, for providing stratigraphic or paleobathymetric information. We also thank N. J. Douglas and B. K. Trujillo for their care in preparing manuscript and illustrations.

REFERENCES

- Bandy O. L., 1953. Ecology and paleoecology of some California Foraminifera. Part II, Foraminiferal evidence of subsidence rates in the Ventura basin, *J. Paleontol.*, **27**, 200-203.
- Berggren W. A., 1972. A Cenozoic time-scale: some applications for regional geology and paleobiogeography, *Lethaia*, **5**, 195-215.
- Bubb J. N., Hatlelid W. G., 1977. Seismic stratigraphy and global changes of sea level, Part 10: Seismic recognition of carbonate buildups, in: *Seismic stratigraphy — application to hydrocarbon exploration*, edited by C. E. Payton, AAPG Mem., **26**, 185-204.
- Hardenbol J., Berggren W. A., 1978. A new Paleogene numerical time scale, *AAPG Stud. Geol.*, **6**, 213-234.
- Hayes D. E., Rabinowitz P. D., 1975. Mesozoic magnetic lineations and the magnetic quiet zone off northwest Africa, *Earth. Planet. Sci. Lett.*, **28**, 105-115.
- Hays J. D., Pitman W. C. III, 1973. Lithospheric plate motion, sea-level changes and climatic and ecological consequences, *Nature*, **246**, 18-22.

- Horowitz D. H.**, 1976. Mathematical modeling of sediment accumulation in prograding deltaic systems, in : *Quantitative techniques for the analysis of sediments*, edited by D. F. Merriam, Proc. IX Int. Sed. Congr., Nice, France, 1975, 105-119.
- Lemoine P.**, 1911. *Géologie du Bassin de Paris*, Librairie Scientifique Herman & fils, Paris.
- Mitchum R. M. Jr., Vail P. R., Thompson S., III**, 1977. Seismic stratigraphy and global changes of sea level, Part 2 : The depositional sequence as a basic unit for stratigraphic analysis, in : *Seismic stratigraphy — application to hydrocarbon exploration*, edited by C. E. Payton, AAPG Mem., **2**, 16, 53-62.
- Pflum C. E., Frerichs W. E.**, 1976. Gulf of Mexico deep-water foraminifers, edited by W. V. Sliter, Cushman Found, *Foraminiferal Res., Spec. Publ.*, **14**, 1-125.
- Pitman W. C. III**, 1978. Relationship between eustacy and stratigraphic sequences of passive margins, *Geol. Soc. Am. Bull.*, **89**, 1389-1403.
- Pitman W. C. III, Talwani M.**, 1972. Sea-floor spreading in the North Atlantic, *Geol. Soc. Am. Bull.*, **83**, 619-646.
- Royden L., Sclater J. G., Von Herzen R. P.**, 1980. Continental margin subsidence and heat flow : important parameters in formation of petroleum hydrocarbons, *AAPG Bull.*, **64**, 173-187.
- Sangree J. B., Widmier J. M.**, 1977. Seismic stratigraphy and global changes of sea level, Part 9 : Seismic interpretation of clastic depositional facies, in : *Seismic stratigraphy — application to hydrocarbon exploration*, edited by C. E. Payton, AAPG Mem., **26**, 165-184.
- Sangree J. B., Widmier J. M.**, 1979. Interpretation of depositional facies from seismic data, *Geophysics*, **44**, 131-160.
- Tipword H. L., Setzer F. M., Smith F. L., Jr.**, 1966. Interpretation of depositional environment in Gulf Coast petroleum exploration from paleoecology and related stratigraphy, *Trans. Gulf Coast. Assoc. Geol. Soc.*, **16**, 119-130.
- Todd R. G., Mitchum R. M. Jr.**, 1977. Seismic stratigraphy and global changes of sea level, Part 8 : Identification of Upper Triassic, Jurassic and Lower Cretaceous seismic sequences in Gulf of Mexico and offshore west Africa, in : *Seismic Stratigraphy — application to hydrocarbon exploration*, edited by C. E. Payton, AAPG Mem., **26**, 145-163.
- Vail P. R., Hardenbol J.**, 1979. Sea-level changes during the Tertiary, *Oceanus*, **22**, 71-79.
- Vail P. R., Mitchum R. M.**, 1980. Global cycles of sea-level change and their role in exploration. *Proc. Tenth World Petroleum Congress*, **2**, Expl. Supply & Demand, 95-104.
- Vail P. R., Todd R. G.**, 1981. Northern North Sea Jurassic unconformities, chronostratigraphy and sea-level changes from seismic stratigraphy, *Proc. Petrol. Geol. Cont. Shelf*, N. W. Europe Conf., in press, Heydon & Son, Philadelphia.
- Vail P. R., Mitchum R. M. Jr., Thompson S. III**, 1977. Seismic stratigraphy and global changes of sea level. Part 3 : Relative changes of sea level from coastal onlap, in : *Seismic stratigraphy — application to hydrocarbon exploration*, edited by C. E. Payton, AAPG Mem., **26**, 63-81.
- Van Hinte J. E.**, 1976 a. A Jurassic time scale, *AAPG Bull.*, **60**, 489-497.
- Van Hinte J. E.**, 1976 b. A Cretaceous time scale, *AAPG Bull.*, **60**, 498-516.
- Van Hinte J. E.**, 1978. Geohistory analysis-application of micropaleontology in exploration geology, *AAPG Bull.*, **62**, 201-222.
- Watts A. B., Ryan W. B. F.**, 1976. Flexure of the lithosphere and continental margins, *Tectonophysics*, **36**, 25-44.
- Watts A. B., Steckler M. S.**, 1979. Subsidence and eustasy at the continental margin of eastern north America, in : *Deep drilling results in the Atlantic ocean : continental margins and paleoenvironment*, edited by M. Talwani, W. F. Hay and W. B. F. Ryan, *Maurice Ewing Ser.*, **3**, 218-234.